scientific reports

Check for updates

OPEN

Liquid biopsy of embryo culture medium for assessing human embryo viability using Raman spectroscopy

Mika Ishigaki[1]✉, Runa Tamano[1], Nao Inagaki[1], Hiromitsu Shirasawa[2], Yukiyo Kumazawa[2], Kazumasa Takahashi[2] & Yukihiro Terada[2]✉

This study investigated the potential of assessing human embryo viability through the analysis of the embryo culture medium used in assisted reproductive technology (ART) via Raman spectroscopy. Two types of culture media—one for early development (medium A) and one for recovery after vitrifying/warming (medium B)—were analyzed. Our results showed that protein concentrations were higher in medium A in which embryos reached the blastocyst stage compared to those in which embryos arrested before this stage. Moreover, the pH of medium A associated with higher-grade blastocysts tended to be more acidic than that associated with lower-grade blastocysts. Conversely, in medium B, pregnancy did not occur even with high-grade blastocysts when the medium was contaminated by residual vitrifying/warming agents or had slightly elevated component concentrations due to water evaporation. Furthermore, medium B tended to be slightly alkaline with higher-grade blastocysts, in contrast to medium A. The noncontact, noninvasive, and label-free Raman spectroscopic method for assessing human embryo viability based on culture media analysis may serve as a liquid biopsy in the near future. As ART has become an important treatment for infertility, this method, which may enhance its safety and efficacy, is expected to contribute to human welfare.

Assisted reproductive technology (ART) has become widespread globally, with more than 70,000 babies born through ART in Japan in 2021, accounting for ~8.6% of all newborns[1]. The success rate of embryo transfer in ART depends on the development potential of the embryo, which can be statistically predicted based on factors such as embryonic morphology and developmental kinetics[2]. Systematic scoring methods for assessing embryo potential have been constructed using extensive data on embryos at the stages of pronuclear, cleavage, and blastocyst[2]. These noninvasive criteria for selecting embryos with high development potential have proven highly effective for improving embryo transfer outcomes. However, these criteria based on the appearance of embryos offer no molecular-level insight into why certain embryos have such developmental potential. Identifying the molecular basis of embryo potential using noninvasive methods is crucial to further improve the success rate of implantation and pregnancy outcome.

One approach to clarifying the correlation between embryo metabolism and developmental potential is studying differences in the composition of the culture medium affected by embryo metabolism. For example, Conaghan et al. investigated whether pyruvate uptake by single embryos from the culture medium on the first, second, and third days after insemination correlated with pregnancy outcomes using ultramicro-fluorescence assays[3]. They found that the mean pyruvate uptake was significantly lower in embryos that implanted than in those that failed to implant. However, uptake variations largely depended on individual embryos, leading to the conclusion that pyruvate uptake alone was insufficient for embryo selection. Gardner et al. further assessed nutrient consumption, including pyruvate and glucose, also using ultramicro-fluorescence assays[4]. They revealed that pyruvate and glucose uptake were substantially higher in embryos that developed into blastocysts compared to those that were arrested before this stage. Furthermore, glucose uptake depended on the grade of blastocysts, and blastocysts with the highest grade showed the highest glucose uptake. Moreover, Kurosawa et al. sought to assess embryonic developmental competency by focusing on the rate of oxygen consumption[5]. In this way, the method of predicting the success rate of ART by analyzing differences in the compositions of the culture

[1]Institute of Agricultural and Life Sciences, Academic Assembly, Shimane University, 1060 Nishikawatsu, Matsue, Shimane, Matsue 690- 8504, Japan. [2]Department of Obstetrics and Gynaecology, Akita University Graduate School of Medicine, 1-1-1, Hondo, Akita-shi, Akita 010- 8543, Japan. ✉email: ishigaki@life.shimane-u.ac.jp; teraday@doc.med.akita-u.ac.jp

medium owing to embryo metabolism can be considered a form of liquid biopsy, akin to diagnosing disease through small amounts of fluid such as blood and saliva. To predict the viability of embryos by analyzing the culture medium as a liquid biopsy in actual ART, it is extremely important to analyze the metabolism of each embryo in real-time in a noninvasive manner while embryos are cultured without sampling.

Raman spectroscopy is a type of vibrational spectroscopy that is similar to infrared spectroscopy. In this spectroscopic analysis, a spectrum is obtained by irradiating a laser onto a sample, dispersing the scattered light, and detecting. This provides information about vibrational modes associated with functional groups in molecules such as proteins, lipids, and DNA/RNA in situ without labeling in a noninvasive and noncontact manner[6,7]. Thus, Raman spectroscopy is suitable for analyzing living organisms, and many studies on its biological and medical applications have been reported[6–9]. In recent years, it has been applied to gamete analysis with the goal of future application in reproductive medicine[10–14]. Wood et al. visualized uneven chemical distributions in mouse oocytes using Raman spectroscopy[10]. They observed distinct differences in the 3050–2780 cm^{-1} region, attributed to C–H stretching vibrations in proteins and lipids, depending on oocyte maturation between the germinal vesicle (GV) and metaphase II (MII) phases, concluding that this wavenumber region could serve as a molecular marker for assessing oocyte maturation. Heraud et al. explored 2D and 3D Raman imaging of living and fixed mouse oocytes[11]revealing differences in lipid composition between their GV and MII stages. Ishigaki et al. have been developing a method to identify female gametes with high probabilities of successful pregnancy outcomes[12–14]. They investigated molecular changes in mouse oocytes over time after ovulation using two excitation wavelengths, 785 and 532 nm, detecting nondestructive variations in lipid and phosphate concentrations, as well as differences in the redox state of cytochrome c[13,14]. Moreover, several research groups have employed Raman spectroscopy to evaluate oocyte metabolism by analyzing changes in the composition of the culture medium. Scott et al. proposed a model to predict embryo viability on day 3 by analyzing media samples[15]. Liang et al. examined differences in the components of the culture medium for aneuploid and euploid embryos[16]. Raman spectroscopy analysis of culture medium offers a less invasive approach, as the laser does not directly irradiate the gametes. If the viability of gametes can be assessed based on the examination of culture medium using Raman spectroscopy, it could serve as a liquid biopsy for predicting pregnancy outcomes.

Herein, culture media used for human embryos were analyzed using Raman spectroscopy to verify whether the differences in the components of culture media owing to embryo metabolism could be detected based on the developmental grade and stage of embryos. Two types of media—one for culturing early embryos up to the blastocyst stage and another for recovering vitrified/warmed blastocysts—were examined. Raman spectra revealed variations in protein concentration and pH of culture media, depending on the developmental stage of the embryos and pregnancy outcomes. Notably, high-grade blastocysts that successfully implanted exhibited less contamination of the culture medium by components from the vitrifying/warming media, suggesting that this approach provides information about the culture conditions. While it is difficult to provide an index for selecting embryos with high pregnancy outcomes using only Raman spectral data, this study shows the possibility of selecting embryos in better conditions among the embryos, even when they are of the same morphological grade. It is expected that noninvasive, nonstaining, real-time liquid biopsies based on embryo culture will improve the success rate of ART.

Materials and methods

Supernatant of embryo culture

Two types of supernatants from in vitro fertilized embryo cultures were analyzed using Raman spectroscopy. Herein, two media are named medium A (HiGROW OVIT, FUSO Pharmaceutical Industried, Ldt., Osaka, Japan) and medium B (EmbryoGlue, Vitrolife K. K., Tokyo, Japan). Medium A was used for developing culture for early embryos, while medium B was for culturing embryos after vitrifying and waring. Four types of culture media for vitrification (VT507-1, VT507-2, KITAZATO, Shizuoka, Japan) and warming (VT508-2, VT508-3, KITAZATO, Shizuoka, Japan) of embryos were used. The culture media generally consists of amino acids (including essential amino acids), salts such as NaCl and KCl, sugars such as glucose and lactate, sodium pyruvate, human serum albumin (HSA), ethylene diamine tetra acetic acid, and phosphate ions (KH_2PO_4 and NaH_2PO_4). Although the ingredients of the two media used in this study are publicly available, detailed information such as their concentrations are not disclosed. ART was performed at the Department of Obstetrics and Gynecology, Akita University Hospital. Each embryo was cultured individually in a 25-µl medium drop (37 °C, 6% CO_2, 5% O_2). After incubation, supernatants from embryo cultures were collected, frozen in microtubes, and transported to Shimane University. The frozen media were thawed at room temperature (~ 25 °C) and subjected to Raman spectroscopic analysis.

Each medium sample was used to culture a single embryo, and the developmental stage and grade of each embryo were recorded alongside pregnancy outcomes. The developmental stage and grade for early embryos was identified using the Veeck classification, while that for blastocysts followed the Gardner classification[17,18]. In the Gardner classification, blastocysts are assigned a numerical score from 1 to 6 to reflect their developmental stage. This is accompanied by alphabetic grades, A to C, which assess the quality of the inner cell mass and trophectoderm based on their morphological properties. A higher numerical score indicates a faster rate of blastocyst expansion, while an "A" grade signifies better quality than a "C" grade[18]. The media samples A were collected from 31 women, with 17 women undergoing conventional in vitro fertilization (cIVF) and 14 women undergoing intracytoplasmic sperm injection (ICSI). Media B samples were obtained from 30 women, with 10 women treated by cIVF and 20 women treated by ICSI. The frozen media were transported from Akita University to Shimane University, along with information about the type of culture media (A or B), the type of infertility treatment used, and the final stage of embryo development, excluding personal information. Some media were selected as reference data, where the embryos were not in optimal condition and their development was arrested. Additionally, some embryos have not been transferred, and their pregnancy outcomes have not yet

been determined. Furthermore, the media samples were collected from women of various ages, including both younger women and older women who had undergone ovarian freezing during breast cancer treatment. However, this study did not explore the relationship between specific factors affecting pregnancy and spectroscopic results. Instead, the focus was on examining differences in culture media based on the embryo grade. The sample sizes for the two types of media, along with the corresponding stages, grades and pregnancy outcomes, are summarized in Table 1, which shows the number of embryos. Control media were kept in the incubator without embryos for five days under the same conditions (37 °C and 5% CO_2) with an oil cover, simulating the environment in which embryos were cultured.

All experiments were approved by the Ethics Committees of Akita University and Shimane University (2704). All methods adhered to institutional guidelines. Informed consent was obtained from donors to donate the culture media used for embryo culture according to the guidelines of the Declaration of Helsinki. All methods were performed in accordance with institutional guidelines.

Raman measurements

Raman measurements of culture media were conducted using a Raman microscope (XploRA INV, HORIBA Ltd., Kyoto, Japan) equipped with a 532 nm diode laser, a spectrometer with an 1800 gr/mm grating, a charge-coupled device camera, and a microscope (Eclipse Ti2 Inverted Microscope, Nikon Co., Tokyo, Japan) with a 40× objective lens (Plan Fluor, NA = 0.6; Nikon). The power of the incident laser light at the sample point was ~ 300 mW, and Raman spectra were calibrated using the peak of silicon. Each thawed medium sample was drawn into a glass capillary (outer diameter: 1.52 mm, inner diameter: 1.13 mm, Drummond Scientific Company, Broomall, PA) and measured under temperature control at 37 °C with a stage heater (monotone-100, ThreeHigh Co., Ltd., Japan). Raman spectra were collected in the 1800–400 cm^{-1} region with an exposure time of 10 s and 60 scan accumulations, leading to a total exposure time of 600 s. Each medium sample was measured twice, with different measurement points. The autofluorescence background was removed using fifth-order polynomial fitting with a custom calculation program. The collected Raman spectra were normalized using the band intensity at ~ 1635 cm^{-1} attributed to water. Principal component analysis (PCA)[19] was conducted on the preprocessed spectral data to extract different spectral components between samples using the chemometrics software Unscrambler X 10.3 (Camo Analytics, Oslo, Norway). In PCA, the axis that maximizes variance among the data is extracted as principal component (PC) 1, while subsequent PCs are determined to maximize variance under the constraint of orthogonality to previously defined PCs. The mean-centered spectral data matrix (W) is expressed as a linear combination of the score (T) and loading (P) vectors of each PC determined in this manner.

$$W = T_1 P_1^T + T_2 P_2^T + T_3 P_3^T + \cdots \quad (1)$$

The score plot of each PC in two or three dimensions allows visualization of systematic differences in variances depending on the groups constructing the spectral data set. The loadings of the corresponding PCs are interpreted as vector components that reflect the systematic differences between groups.

Statistical analysis

A comparative analysis of multiple groups was performed using one-way analyses of variance (ANOVA) with Tukey's method. To evaluate statistically significant differences between the mean values of the two groups, the Student's t-test was adopted. A threshold p-value of 0.05 was established to determine the existence of significant differences.

Results and discussion

Figure 1a shows the mean Raman spectra in the 1800–600 cm^{-1} region for the two types of control culture media A and B used in this study. The most intense Raman band observed at 1635 cm^{-1} results from the O–H bending mode of water, overlapping with the amide I mode band in proteins[20,21]. The bands observed at 1450 and 1416 cm^{-1} are assigned to the C–H deformation in proteins, amino acids, and saccharides, while the broad feature around 1300 cm^{-1} comes from the overlapping of amide III mode and CH_3/CH_2 twisting and bending modes of proteins and amino acids[22]. The striking intense bands located at 1002 cm^{-1} are attributed to the

a								
Stage and Grade	**Ctrl**	**unF**	**deg frag**	**2-cell**	**4-cell**	**8-cell**	**3AA-3CC**	**4AA-4CC**
Sam. Num.	5	5	11	1	2	2	20(11)	17(16)
Pregnancy	0	0	0	0	0	0	2(1)	1(1)

b					
Stage and Grade	**Ctrl**	**3AA-3CC**	**4AA-4CC**	**5AA-5CC**	**6AA**
Sam. Num.	4	2(1)	12(6)	24(22)	1
Pregnancy	0	0	1(1)	4(4)	0

Table 1. (**a**) and (**b**) sample numbers of culture media A and B, respectively, for each stage and grade, including the corresponding pregnancy outcomes. The numbers in parentheses indicate the sample numbers graded without a grade of C for the inner cell mass and trophectoderm, such as AA, AB, BA, and BB. Sam. Num.: number of samples, Ctrl: control, unF: unfertilized, deg: degenerated, frag: fragmented.

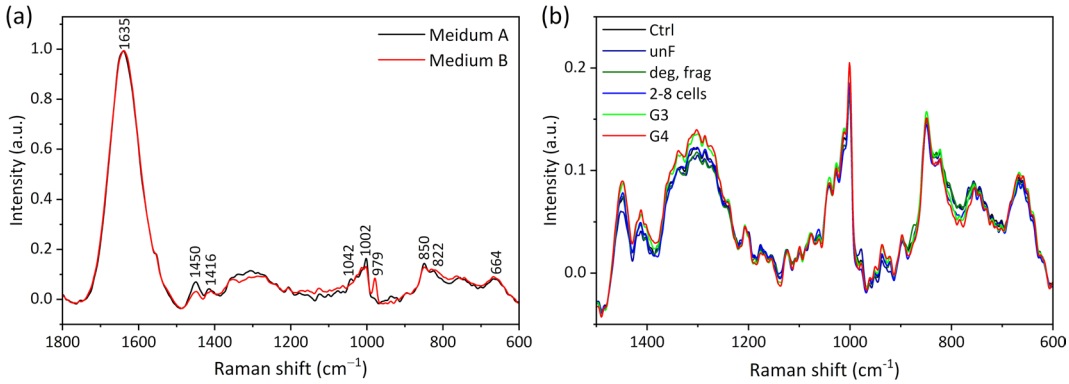

Fig. 1. (**a**) Mean Raman spectra in the 1800–600 cm^{-1} region for the two control culture media used in this study, with media A designated for developmental culture and medium B for recovery culture. (**b**) Mean Raman spectra in the 1500–600 cm^{-1} region for medium A, comparing the control spectra with those at different developmental stages.

Band (cm^{-1})	Assignment
664	C-C twi
822	ring br Tyr
850	ring br Tyr
979	ring br Thia
1002	sym ring br Phe
1260–1300	Amide III, CH_2 def
1416	CH def
1450	CH def
1635	Amide I, O-H ben

Table 2. Band assignments of averaged Raman spectra of culture medium[22–24]. sym: symmetric, twi: twisting, br: breathing, def: deformation, str: stretching, ben: bending, Phe: Phenylalanine, Try: Tryptophan, Thia: Thiazole.

symmetric ring breathing mode of phenylalanine[22–24]. Another standout band at 979 cm^{-1} was observed in the spectrum of medium B. Among the components present only in medium B, such as pyridoxine, riboflavin, thiamine, and hyaluronic acid, thiamine exhibits a strong Raman band at 979 cm^{-1} owing to the ring breathing mode of thiazole[25]. The doublet bands observed at 850 and 822 cm^{-1} originate from the ring-breathing vibrational mode of tyrosine[22,26]. The assignment of the bands is summarized in Table 2. The Raman spectra of the culture media in Fig. 1a reflected spectral patterns corresponding to the medium constituents such as amino acids, sugars, salts, and proteins.

Developmental culture medium (Medium A)

Figure 1b shows the mean Raman spectra in the 1500–600 cm^{-1} region for medium A, used as control, and those used for embryonic development. Among these, some samples halted embryonic development, categorized as unfertilized (unF), degenerated (deg), and fragmented (frag), while the others proceeded to different developmental stages, including 2–8 cells and blastocysts graded as 3 (G3) and 4 (G4). To investigate the differences in the components of culture media resulting from the metabolisms of embryonic development, PCA was conducted on the Raman spectral data in the 1800–600 cm^{-1} region collected from the control medium and those used for culturing embryos that developed into the G3 or G4 blastocysts. Figure 2a and b depict the plots of scores (PC 1 vs. PC 2) and the loading plot for PC 1, respectively. The control data tended to cluster separately in the negative range for PC 1, while the other data groups were plotted in the positive. The PCs with higher order were confirmed not to contribute to the separation of the data into groups. In the loading plot of PC 1, bands at 1653, 1447, 1339, 1301, 1045, 1001, 937, and 849 cm^{-1} were observed positively along the y-axis. They were assigned to the amide I (1653 cm^{-1}), C–H deformation (1447 cm^{-1}), CH_3/CH_2 twisting and bending (1339 and 1301 cm^{-1}), phenylalanine (1045 and 1001 cm^{-1}), C–C stretching (937 cm^{-1}), and tyrosine (849 cm^{-1}), where the combination of these bands is characteristic of the spectral pattern collected from general protein samples. For reference, a Raman spectrum of human serum albumin (HSA) is shown in Figure S1 in the Supporting Information (SI 1) as one example of proteins. The positive bias of PC 1 scores for the G3 and G4 data suggests that the concentration of proteins within culture media where oocytes developed into high-grade blastocysts was higher than in the control, owing to embryonic metabolism. Box plots of the PC 1 scores in Fig. 2c indicate that the concentration of proteins was higher in the culture media with G4 blastocysts compared to those with

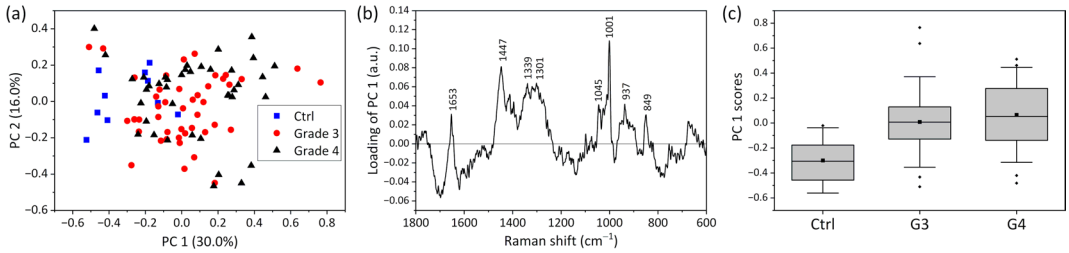

Fig. 2. (**a**) Score plots (PC 1 vs. PC 2) and (**b**) loading plot of PC 1. (**c**) Box blots of PC 1 scores. The box represents the interquartile range (IQR = $Q_{3/4} - Q_{1/4}$), with ▪ indicating the mean, ◆ marking outliers, the central line showing the median, and error bars representing ± 1.0 standard deviation (SD).

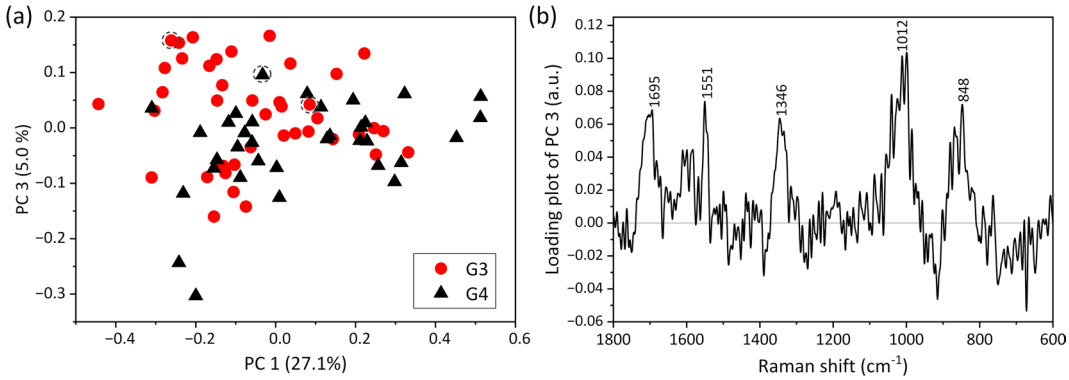

Fig. 3. (**a**) Score plots (PC 1 vs. PC 3) and (**b**) loading plots of PC 3, extracted from PCA on the spectral data of G3 and G4 blastocysts.

G3. The box plots of PC 1 scores based on the detailed embryo grade are shown in Figure S2. This suggests that the higher protein concentrations in the culture media supporting the development of G3 and G4 blastocysts are a result of embryonic metabolism. Furthermore, PCA conducted on the dataset, including control media and those where embryos did not develop (unfertilized, degenerated, and fragmented) or developed only to 2–8 cells, did not yield PCs that separated the data into distinct groups (Figure S3). Zygotic genome activation starts from 8-cell stage in human embryos, indicating that embryo metabolism increases after the stage[27]. By taking the prior knowledge into account, the result seems reasonable.

Here, we discuss the possibility of identifying the protein species whose concentrations increase owing to embryonic metabolism. The Raman spectrum of HSA in Figure S1 of SI 1 shows similar spectral patterns in the loading plot of PC 1, albeit with variations in relative band intensities. These spectral patterns are typical of general proteins, making it challenging to identify specific protein species unless they possess a very distinctive molecular structure. For example, some proteins contain chromophores, allowing for high sensitivity and selectivity identification of molecular structures through the resonance Raman effect. Heme proteins are well-known examples of this phenomenon[28,29]. Characteristic Raman bands corresponding to C = C and C–C stretching vibrations of porphyrin are strongly detected in the 1700–1300 cm^{-1} region when using an excitation wavelength in the ultraviolet–visible (UV–vis) wavelength region. However, the loading of PC 1 did not show such characteristic properties. Furthermore, we considered the potential for detecting early secretion of the human chorionic gonadotrophin (hCG) hormone from the blastocyst. The secretion of hCG by cultured human blastocysts is reported to begin around day 7 of development[30,31]. The Raman spectrum in the 1800–600 cm^{-1} region of the hCG solution is shown in Figure S1; it features a striking band at 989 cm^{-1}, along with small bands at 1077 and 850 cm^{-1}. As a glycoprotein, the spectrum pattern of hCG is very similar to that of erythropoietin secreted from the kidney[32]. However, it is unclear whether the spectral patterns characteristic of glycoproteins are represented in the loading of PC1. Thus, the specific protein species cannot be determined from the loading of PC 1. However, the increase in protein concentration in culture media suggests that the metabolic activity of embryos may serve as an indicator for evaluating embryonic viability.

Furthermore, PCA was conducted to the dataset, including only G3 and G4 blastocysts. Figure 3a depicts the score plots of PC 1 vs. PC 3, where the data were roughly classified into two groups. Notably, the G4 data were unevenly distributed in the negative region for PC 3, while the other PCs did not contribute to separating the data into distinct groups. The data points in the score plots enclosed in dotted circles express culture media in which the cultured blastocysts successfully led to pregnancies after implantation. No PC characteristics of the culture medium that led to pregnancy were extracted. The PC 1 loading showed the same spectral patterns characteristic of proteins shown in Fig. 2b, and the scores of PC 1 for G4 blastocysts were larger than those for G3, as previously discussed. In the loading plots of PC 3 (Fig. 3b), a broad peak at ~ 1012 cm^{-1} was observed,

revealing that the Raman spectra of culture media with G4 blastocysts exhibited lower intensity at this frequency compared to those of G3.

To identify the components within the culture media responsible for the spectral changes shown in Fig. 3b, the control medium was perturbed by changing the pH from 5 to 9 using HCl or NaOH addition. Figure 4a shows the Raman spectra in the 1500–600 cm^{-1} region of medium A with varying pH levels. PCA was conducted on the dataset of the culture medium to extract the spectral components that changed with pH variations. Figure 4b depicts the score plots of PC 1 against pH, clearly revealing a characteristic pattern: PC 1 scores increased as pH increased from 5 to around 8 but decreased as pH further increased from 8 to 9. The loading plots of PC 1 in Fig. 4c showed peaks at 1555, 1356, 1015, and 830 cm^{-1}. This pattern was very similar to that of PC 3 shown in Fig. 3b, except for the peak at 1695 cm^{-1}. Thus, the spectral differences between the culture media with G3 and G4 blastocysts were mainly attributed to the spectral components associated with pH variations in the culture media.

Medium A includes potassium dihydrogen phosphate, and the neutralization reaction of phosphate ions acts as a pH buffer. Figure 4d depicts the titration curve of the culture medium upon adding HCl or NaOH to medium A. Three neutralization points were observed, and the pH rapidly changed at 4.0–6.0, 7.5–9.3, and 11.0–11.7. The main pH ranges between 5 and 9, including the physiological pH of around 7.0, which corresponds to the pH range between the first and second neutralization points. At the second neutralization point, the phosphate ion changes from $H_2PO_4^-$ to HPO_4^{2-} as pH increases. Specifically, the concentration of $H_2PO_4^-$ increases as pH increases from 5.0 to 7.5, then decreases rapidly in the higher pH range from 7.5 to 9.0. The variation in PC 1 scores in Fig. 4b mirrors the concentration change of $H_2PO_4^-$. Thus, the spectral component expressed by PC 1 in Fig. 4b and c effectively captures the concentration variation of $H_2PO_4^-$, while PC 3 in Fig. 3b corresponds to the spectral variation caused by pH changes in medium A owing to embryo metabolism. The PCA results for embryo culture in Fig. 3a reveal that the PC 3 scores of G4 blastocysts tend to be lower than those of G3, as previously discussed. Generally, embryo culture media are maintained at pH ~ 7.0 in a CO_2 incubator. This suggests that the concentration of $H_2PO_4^-$ in the G4 medium is lower than in G3, indicating that the G4 culture medium is slightly more acidic than that of G3. A detailed discussion of the Raman spectral variations of the culture medium associated with the pH changes is developed in SI 2 (Figures S4 and S5). Lactate production has been reported throughout the development of human preimplantation embryos[33]suggesting that the culture media with G4 blastocysts may have become acidic owing to the influence of such acidic substances.

To quantitatively evaluate pH variations in culture media, PC 1 scores were derived by applying the Raman spectral dataset obtained from human embryo culture as a validation set to the model shown in Fig. 4b and c, which was constructed based on the dataset from culture media where the pH was artificially changed. A detailed analysis of the pH variations in culture media is provided in SI 2. Figure 5a depicts the plot of sample number vs. PC 1 scores, revealing that the scores were distributed between − 0.1 and 0.4. Referring to Fig. 4b,

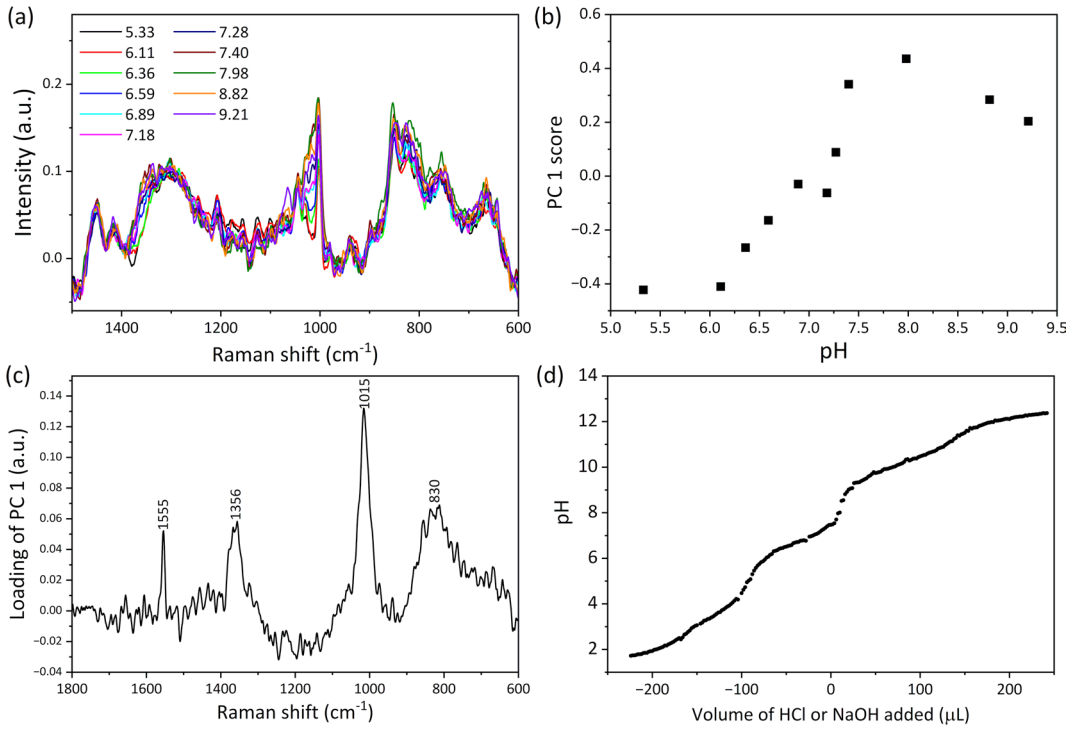

Fig. 4. (**a**) Raman spectra in the 1500–600 cm^{-1} region for control culture medium A with pH values ranging from 5 to 9. (**b**) Plot of PC 1 scores vs. pH and (**c**) loading plot of PC 1 from PCA. (**d**) Titration curve of the culture medium with 1.0 mol/L HCl or NaOH. Positive and negative *x*-axis values represent the volumes of NaOH and HCl added, respectively.

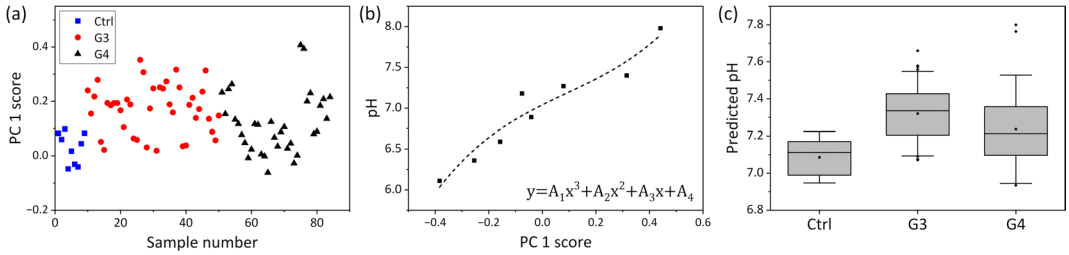

Fig. 5. (**a**) Plot of sample number vs. PC1 scores. (**b**) Calibration curve for predicting pH from PC 1 scores, fitted using a third-order polynomial with four real numbers: $A_1 = 3.96$, $A_2 = -1.05$, $A_3 = 1.64$, and $A_4 = 7.04$. The model demonstrated high accuracy with an R^2 value of 0.93. (**c**) Box plot of predicted pH, where the box represents the interquartile range ($IQR = Q_{3/4} - Q_{1/4}$), ▪ indicates the mean, ◆ marks outliers, the central line represents the median, and the error bars represent ± 1.0 SD.

these PC1 values correspond to a pH range of 7.0–7.4. Moreover, the PC 1 scores for G4 tended to be lower than those for G3. Figure 5b shows the calibration curve for predicting the pH of culture media from PC 1 scores, constructed based on the data in Fig. 4b using third-order polynomials. The model was successfully established with high accuracy, as indicated by a squared correlation coefficient (R^2) of 0.93. The pH values were predicted by applying the PC 1 scores from Fig. 5a to the calibration curve. The model suggested that the pH in the G4 culture was more acidic than in G3, based on the prediction using PC 1 scores (Fig. 5c).

Thus, it was found that the effects of embryo metabolism appeared in medium A through variations in protein concentration and pH, and the magnitude of these changes varies depending on the grade of the blastocysts.

Recovery culture medium (Medium B)

Figure 6a depicts the mean Raman spectra in the 1500–600 cm^{-1} region of the medium B used for culturing embryos after vitrifying and warming. A similar spectral analysis was conducted on the medium B, including the control and those used for culturing blastocysts with G3, G4, G5, and G6. Figure 6b and c depict the score plots of PC 1 vs. PC 3 and PC 2 vs. PC 4, respectively. Figure 6b shows that some points for G3–G6 about PC 1 were significantly different from the others. The loading plot of PC 1 (Fig. 6d) exhibited the spectral pattern of the medium used to warm vitrified embryos (Figure S6 in SI 3), indicating that PC 1 captured the spectral component associated with the culture media used for warming vitrified embryos. The outliers for PC 1 did not result in pregnancy, which may suggest that the media used for warming is better to be free from contamination. However, the remnant of the warming medium is not the sole cause of implantation failure, as other uncertain factors may also contribute. In Fig. 6c, the dataset was classified into two groups as control and cultured media based on PC 2 and PC 4. The data points of pregnancy were biased toward the negative for PC 2 and plotted negatively for PC 4, in contrast to the main data points of control plotted positively. The loading plot of PC 2 in the 1020–970 cm^{-1} showed spectral patterns similar to those of the control culture medium B in Fig. 1. In this study, all Raman spectra were normalized using the band intensity at ~ 1635 cm^{-1} attributed to water. Thus, this suggests that the concentration of the medium B used for culturing blastocysts slightly increased owing to the evaporation of water. As the distribution of the PC 2 scores for pregnancy data resembled that of the control, the concentration of the media B containing embryos leading to pregnancy did not change significantly. The increase in concentration of culture media owing to the evaporation of water may alter the osmotic pressure on the cells, leading to harmful conditions for cells. In the loading plot of PC 4 in Fig. 6d, a characteristic waveform is observed at around 980 cm^{-1}, with peaks at 980 cm^{-1} (positive) and at 997 and 972 cm^{-1} (negative). The zigzag peaks in such a narrow wavenumber region indicate a peak shift at ~ 980 cm^{-1}. Furthermore, the scores of PC 4 were positively distributed only for the control medium (Fig. 6c). The biased distribution of PC 4 exhibited significant differences between the control medium and the medium used for embryo culture, as determined by one-way ANOVA with Tukey's method (Figure S7a). These results indicate that the peaks may systematically shift for the medium where blastocysts were cultured, especially in the medium with pregnancy compared to the control. To confirm the insights from the PCA results, the mean Raman spectra were compared between control, G3–G4 (not pregnant), G5–G6 (not pregnant), and the pregnancy groups among G4 and G5 (Figures S7b and S7c). Figure S7c shows that the Raman band at ~ 980 cm^{-1} certainly shifted to a lower wavenumber for the culture medium, especially for that associated with pregnancy. Even though the magnitude of the band shifts was small (~ 2 cm^{-1}), particularly for the medium with pregnancy, these shifts were statistically significant. However, the causes of the band shift remain unclear.

One-way ANOVA with Tukey's method was also conducted on the PC 3 scores (Figure S7d). The control exhibited statistically significant differences compared to the G5–G6 and pregnancy groups. The loadings of PC 3 in Fig. 6d showed common peaks with those of PC 1 related to the spectral variations caused by pH changes in the culture medium (Fig. 3b), except for the overlapping peaks represented by PC 1 in Fig. 6d, which were owing to the medium used for thawing vitrified embryo. In the G5–G6 and pregnancy groups, the PC 3 scores were larger than those of the other groups. This indicates that PC 3 in Fig. 6d reflects the spectral component derived from pH variations in medium B, with pH levels of the media used for culturing blastocysts, especially those leading to higher–grade blastocysts and pregnancy, tending to become alkaline. The trend of pH variations in medium B contrasts with that observed in medium A explained in the previous subsection. This pH change may result from alkaline substances such as ammonia produced through embryo metabolism. Interestingly, the pH

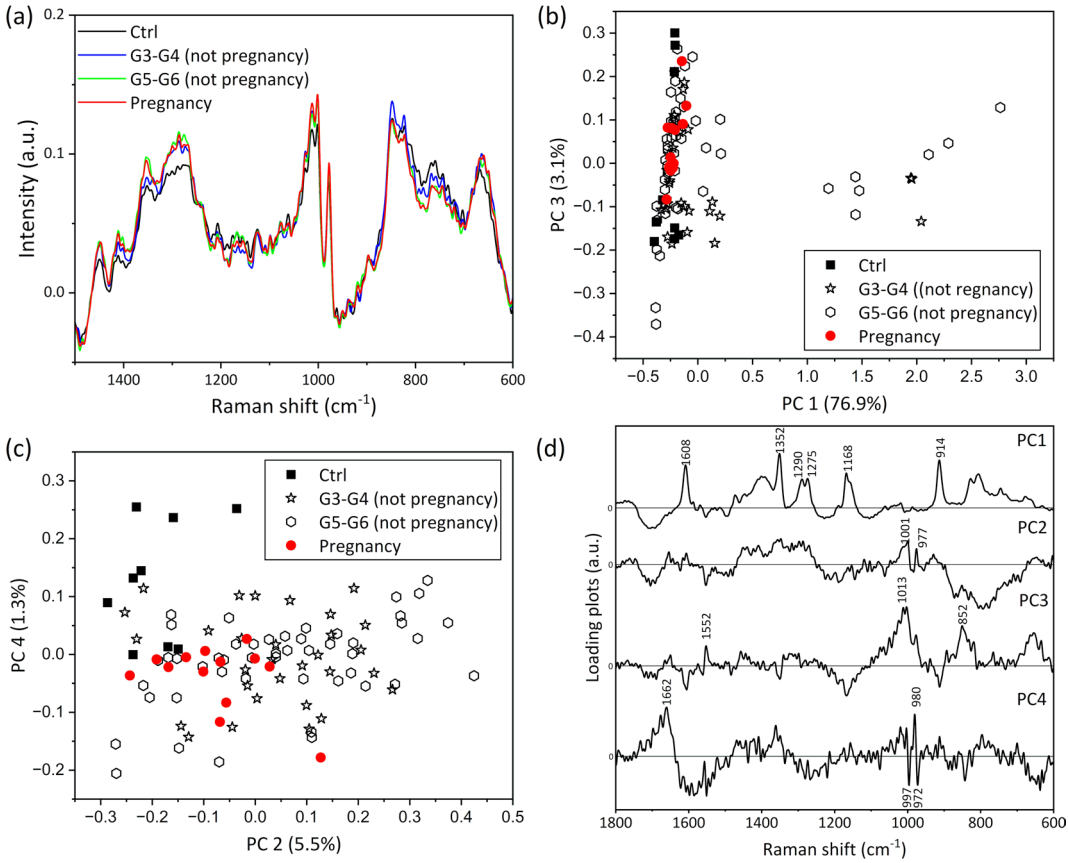

Fig. 6. (**a**) Mean Raman spectra in the 1500–600 cm^{-1} region of medium B for control and across the developmental stages of blastocysts. Score plots of (**b**) PC 1 vs. PC 3 and (**c**) PC 2 vs. PC 4. (d) Loading plots of PCs extracted via PCA from the spectral data for G3–G6.

properties of culture media A and B show opposite trends despite the incubation of higher-graded blastocysts in both cases. Overall, these results highlight the high potential of this method for evaluating pH in microdroplets, which could represent a breakthrough in ART for assessing embryo viability and culturing environments.

Conclusion

Two types of culture media were analyzed using Raman spectroscopy: medium A, used for developing embryos into blastocysts, and medium B, used for recovering vitrified/warmed blastocysts. In medium A, the protein concentration increased in media supporting higher-graded blastocysts, and the pH tended to be more acidic compared to media for lower-graded blastocysts. In contrast, the medium used for warming vitrified blastocysts was not mixed with medium B in cases that led to pregnancy. Furthermore, pregnancy outcomes were found to be lower in culture media where the concentration of components increased due to water evaporation. This may be due to the toxicity of medium used for warming vitrified embryos to the cells and/or changes in osmotic pressure on the cells caused by concentration variations in the culture medium. Moreover, the pH of medium B appeared to be more alkaline with higher-graded blastocysts. The differences in composition and pH of the culture medium were attributed to embryo metabolism, and the magnitude of these differences increased depending on the developmental stage and grade of the blastocysts. This suggests that Raman spectroscopy has the potential to evaluate the viability and pregnancy outcomes by monitoring the culture medium in real-time. Specifically, spectral variations caused by artificially induced pH changes in the culture medium were detected in the media used for culturing blastocysts. Measuring the pH of culture media with a pH meter is impractical because of the small volume (~ 20 µL) of the medium. Additionally, indicators such as phenolsulfonphthalein cannot be used in oocyte/embryo culture to avoid the risk of cytotoxicity. Therefore, it is virtually impossible to directly measure and/or assess the pH of the embryo culture media. Thus, Raman spectroscopy can be considered the only method to evaluate the pH of the culture medium in a noncontact, noninvasive, and nonstaining manner. This method for assessing the pH of embryo culture medium can also be applied to other media containing phosphate ions that act as a buffer for culturing somatic cells, embryonic stem cells, and induced pluripotent stem cells. Furthermore, a confocal laser can be irradiated onto the culture medium, allowing for noninvasive, noncontact acquisition of Raman spectra while culturing embryos. For example, embedding Raman spectroscopic mechanism into a time-lapse monitoring system can enable to assess the embryonic potential based on the molecular variations in culture medium in addition to the consecutive observations of embryonic development. The study is a pilot test to determine whether the embryo stage and grade can be evaluated based on differences in the composition

of culture medium using Raman spectroscopy. It is not intended to identify critical values, such as protein concentration and pH, that could predict embryo implantation. However, it is necessary to establish these thresholds for predicting embryo implantation by analyzing more culture media in order to advance ART in the future. Once this is achieved and the safety of laser irradiation on the culture medium is confirmed, real-time monitoring of culture medium using Raman spectroscopy during embryo culture could open a new era for supporting ART, serving as a novel "liquid biopsy" method.

Data availability

The data that support the findings of this study are available from the corresponding author upon reasonable request.

Received: 19 November 2024; Accepted: 8 July 2025
Published online: 30 September 2025

References

1. Katagiri, Y. et al. Assisted reproductive technology in japan: A summary report for 2020 by the ethics committee of the Japan society of obstetrics and gynecology. *Reprod. Med. Biol.* **22**, e12494 (2023).
2. Ezoe, K., Takahashi, T., Miki, T. & Kato, K. Developmental perturbation in human embryos: clinical and biological significance learned from time-lapse images. *Reprod. Med. Biology*. **23**, e12593 (2024).
3. Conaghan, J., Hardy, K., Handyside, A. H., Winston, R. M. & Leese, H. J. Selection criteria for human embryo transfer: a comparison of pyruvate uptake and morphology. *J. Assist. Reprod. Genet.* **10**, 21–30 (1993).
4. Gardner, D. K., Lane, M., Stevens, J. & Schoolcraft, W. B. Noninvasive assessment of human embryo nutrient consumption as a measure of developmental potential. *Fertil. Steril.* **76**, 1175–1180 (2001).
5. Kurosawa, H. et al. Development of a new clinically applicable device for embryo evaluation which measures embryo oxygen consumption. *Hum. Reprod.* **31**, 2321–2330 (2016).
6. Choo-Smith, L. P. et al. Medical applications of Raman spectroscopy: from proof of principle to clinical implementation. *Biopolymers* **67**, 1–9 (2002).
7. Mulvaney, S. P. & Keating, C. D. Raman spectroscopy. *Anal. Chem.* **72**, 145–158 (2000).
8. Ozaki, Y., Baranska, M., Lednev, I. & Wood, B. *Vibrational spectroscopy in protein research*. (Elsevier, Massachusetts, USA, (2020).
9. Carey, P. *Biochemical Applications of Raman and Resonance Raman Spectroscopes* (Elsevier, 2012).
10. Wood, B. R. et al. Shedding new light on the molecular architecture of oocytes using a combination of synchrotron fourier transform-infrared and Raman spectroscopic mapping. *Anal. Chem.* **80**, 9065–9072 (2008).
11. Heraud, P. et al. Label-free in vivo Raman microspectroscopic imaging of the macromolecular architecture of oocytes. *Sci. Rep.* **7**, 8945 (2017).
12. Ishigaki, M., Hashimoto, K., Sato, H. & Ozaki, Y. Non-destructive monitoring of mouse embryo development and its qualitative evaluation at the molecular level using Raman spectroscopy. *Sci. Rep.* **7**, 43942 (2017).
13. Ishigaki, M., Hoshino, Y. & Ozaki, Y. Phosphoric acid and phosphorylation levels are potential biomarkers indicating developmental competence of matured oocytes. *Analyst* **144**, 1527–1534 (2019).
14. Ishigaki, M., Kashiwagi, S., Wakabayashi, S. & Hoshino, Y. In situ assessment of mitochondrial respiratory activity and lipid metabolism of mouse oocytes using resonance Raman spectroscopy. *Analyst* **146**, 7265–7273 (2021).
15. Scott, R. et al. Noninvasive metabolomic profiling of human embryo culture media using Raman spectroscopy predicts embryonic reproductive potential: a prospective blinded pilot study. *Fertil. Steril.* **90**, 77–83 (2008).
16. Liang, B. et al. Raman profiling of embryo culture medium to identify aneuploid and euploid embryos. *Fertil. Steril.* **111**, 753–762 (2019).
17. Veeck, L. L. et al. Maturation and fertilization of morphologically immature human oocytes in a program of in vitro fertilization. *Fertil. Steril.* **39**, 594–602 (1983).
18. Gardner, D. K., Lane, M., Stevens, J., Schlenker, T. & Schoolcraft, W. B. Blastocyst score affects implantation and pregnancy outcome: towards a single blastocyst transfer. *Fertil. Steril.* **73**, 1155–1158 (2000).
19. Jolliffe, I. T. & Cadima, J. Principal component analysis: a review and recent developments. *Philos. Trans. Royal Soc. A*. **374**, 20150202 (2016).
20. Murphy, W. F. & Bernstein, H. J. Raman spectra and an assignment of the vibrational stretching region of water. *J. Phys. Chem.* **76**, 1147–1152 (1972).
21. Seki, T. et al. The bending mode of water: A powerful probe for hydrogen bond structure of aqueous systems. *J. Phys. Chem. Lett.* **11**, 8459–8469 (2020).
22. Movasaghi, Z., Rehman, S. & Rehman, I. U. Raman spectroscopy can detect and monitor cancer at cellular level: analysis of resistant and sensitive subtypes of testicular cancer cell lines. *Appl. Spectrosc. Rev.* **42**, 493–541 (2007).
23. Atkins, C. G., Buckley, K., Blades, M. W. & Turner, R. F. Raman spectroscopy of blood and blood components. *Appl. Spectrosc.* **71**, 767-793 (2017).
24. Wood, B. R. & McNaughton, D. Raman excitation wavelength investigation of single red blood cells in vivo. *J. Raman Spectrosc.* **33**, 517-523 (2002).
25. Ibáñez, D., Pérez-Junquera, A., González-García, M. B., Hernández-Santos, D. & Fanjul-Bolado, P. Spectroelectrochemical Elucidation of B vitamins present in multivitamin complexes by EC-SERS. *Talanta* **206**, 120190 (2020).
26. Siamwiza, M. N. et al. Interpretation of the doublet at 850 and 830 cm^{-1} in the Raman spectra of Tyrosyl residues in proteins and certain model compounds. *Biochemistry* **14**, 4870–4876 (1975).
27. Svoboda, P. Mammalian zygotic genome activation. *Semin Cell. Dev. Biol.* **84**, 118–126 (2018).
28. Chatot, C. L., Ziomek, C. A., Bavister, B. D., Lewis, J. L. & Torres, I. An improved culture medium supports development of random-bred 1-cell mouse embryos in vitro. *Reproduction* **86**, 679–688 (1989).
29. Gardner, D. K. & Lane, M. Culture systems for the human embryo. In *Textbook of Assisted Reproductive Techniques* (eds Gardner, D. K. et al.) 242–266 (CRC, 2017).
30. Hay, D. L. & Lopata, A. Chorionic gonadotropin secretion by human embryos in vitro. *J. Clin. Endocr. Metab.* **67**, 1322–1324 (1988).
31. Lopata, A. & Oliva, K. Chorionic gonadotrophin secretion by human blastocysts. *Hum. Reprod.* **8**, 932–938 (1993).
32. Ishigaki, M., Hitomi, H., Ozaki, Y. & Nishiyama, A. Exposing intracellular molecular changes during the differentiation of human-induced pluripotent stem cells into erythropoietin-producing cells using Raman spectroscopy and imaging. *Sci. Rep.* **12**, 20454 (2022).
33. Gott, A. L., Hardy, K., Winston, R. M. L. & Leese, H. J. Non-invasive measurement of pyruvate and glucose uptake and lactate production by sigle human preimplantation embryos. *Hum. Reprod.* **5**, 104–108 (1990).

Acknowledgements
This study was supported by JSPS KAKENHI Grant Number 23K26679 (M.I. and Y.T.).

Author contributions
M.I., K.T., and Y.T. planned the research. All medical treatments including ART were conducted by H.S., Y. K., and K.T. M.I., R.T., and N.I. carried out the Raman measurements and data analysis. M.I., K.T., and Y.T. discussed all results in detail from the medical and spectroscopic standpoints, and M.I. wrote the main text. All authors discussed the results and approved the manuscript for publication.

Declarations

Competing interests
The authors declare no competing interests.

Additional information
Supplementary Information The online version contains supplementary material available at https://doi.org/10.1038/s41598-025-11195-4.

Correspondence and requests for materials should be addressed to M.I. or Y.T.

Reprints and permissions information is available at www.nature.com/reprints.

Publisher's note Springer Nature remains neutral with regard to jurisdictional claims in published maps and institutional affiliations.